A Graphene-Based Biosensing Platform Based on the Release of DNA Probes and Rolling Circle Amplification

Meng Liu,[†,‡] Jinping Song,[†,§] Shaomin Shuang,[§] Chuan Dong,[§] John D. Brennan,[‡] and Yingfu Li[†,‡,*]

[†]Department of Biochemistry and Biomedical Sciences, McMaster University, 1280 Main Street West, Hamilton, Ontario, L8S 4K1 Canada, [‡]Biointerfaces Institute and Department of Chemistry & Chemical Biology, McMaster University, Hamilton, Ontario, L8S 4M1 Canada, and [§]Institute of Environmental Science, Shanxi University, Taiyuan, 030006 People's Republic of China

ABSTRACT We report a versatile biosensing platform capable of achieving ultrasensitive detection of both small-molecule and macromolecular targets. The system features three components: reduced graphene oxide for its ability to adsorb single-stranded DNA molecules nonspecifically, DNA aptamers for their ability to bind reduced graphene oxide but undergo target-induced conformational changes that facilitate their release from the reduced graphene oxide surface, and rolling circle amplification (RCA) for its ability to amplify a primer-template recognition event into repetitive sequence units that can be easily detected. The key to the design is the tagging of a short primer to an aptamer sequence, which results in a small DNA probe that allows for both effective probe adsorption onto the reduced graphene oxide surface to mask the primer domain in the absence of the target, as well as efficient probe release in the presence of the target to make the primer available for template binding and RCA. We also made an observation that the circular template, which on its own does not cause a detectable level of probe release from the reduced graphene oxide, augments target-induced probe release. The synergistic release of DNA probes is interpreted to be a contributing factor for the high detection sensitivity. The broad utility of the platform is illustrated though engineering three different sensors that are capable of achieving ultrasensitive detection of a protein target, a DNA sequence and a small-molecule analyte. We envision that the approach described herein will find useful applications in the biological, medical, and environmental fields.

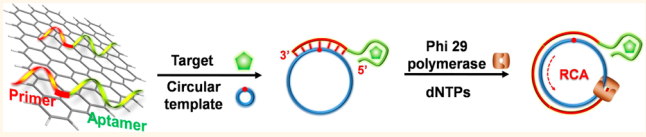

KEYWORDS: aptamer · biosensor · reduced graphene oxide · molecular beacon · rolling circle amplification

The development of simple, ultrasensitive, highly selective and cost-effective biosensing platforms is essential for biological assays and clinical diagnostics. Due to their unique physicochemical properties, nanomaterials possess the ability to facilitate signal transduction and amplify molecular recognition events,[1−3] which makes them ideal candidates in the design of biosensing systems with advanced functions.

Recently, it has been demonstrated that graphene-based nanomaterials can function as excellent transducing elements due to their fascinating physical and chemical characteristics.[4−9] For example, the existence of π-rich conjugation domains gives graphene the ability to interact with single-stranded DNA (ssDNA) molecules via $\pi-\pi$ stacking interactions.[10] With the use of suitable DNA molecules as molecular recognition elements (such as DNA aptamers), the conjugated graphene materials can be used for biosensing. Many DNA−graphene based optical biosensors have been designed for the detection of targets that include DNA,[11−13] microRNA,[14] metal ions,[15] small molecules,[16,17] and proteins.[18,19]

A limitation of conventional DNA−graphene based sensors is their relatively poor sensitivity. In response, several groups have developed cyclic enzymatic amplification strategies to amplify the signals in order to achieve ultrasensitive detection of targets like small molecules (ATP and cocaine) and DNA.[20−22] These designs rely on target recycling carried out by a particular nuclease (such as DNase I) through the digestion of the DNA aptamer. However, for macromolecular targets (such as proteins), the target recycling process cannot be initiated by a nuclease as steric hindrance prevents the nuclease from efficiently digesting the aptamer.[23,24] Thus, a great challenge that remains is how to devise amplification strategies that are highly compatible with graphene materials and broadly applicable for wide ranging targets.

* Address correspondence to liying@mcmaster.ca.

Received for review December 15, 2013 and accepted May 24, 2014.

Published online May 25, 2014
10.1021/nn5007418

It is well-known that rolling circle amplification (RCA) is an advanced isothermal DNA replication process that has the ability to generate DNA products with thousands of tandem sequence repeats,[25] and thus RCA can be exploited as a powerful signal amplification tool to derive amplified biosensors.[26−29] However, to date RCA has not been explored as a signal amplification strategy in the design of graphene-based biosensors. In this study, we report a strategy in which the RCA process is uniquely exploited to amplify molecular recognition events occurring on the surface of reduced graphene oxide.

RESULTS AND DISCUSSION

We first synthesized graphene oxide using a modified Hummers method previously described.[30] Atomic force microscopy (AFM) in Figure 1A revealed that the resultant graphene oxide had an average height of 10 Å, indicating the formation of the single layered graphene oxide.[31] We then converted graphene oxide to reduced graphene oxide through chemical reduction using L-ascorbic acid. Two fundamental vibrations are observed in the Raman spectra of reduced graphene oxide (Figure 1B): the D-band at 1336 cm^{-1} and the G-band at 1590 cm^{-1}. In addition, the D/G ratio increased after the reduction, suggesting that more sp^2 domains were formed, similar to the observation with graphene sheets prepared by hydrazine reduction.[32] The reduction of graphene oxide was further characterized using X-ray photoelectron spectroscopy (XPS). From the C 1s XPS spectrum of graphene oxide (Figure 1C), four different peaks, centered at 284.5, 286.4, 287.8, and 289.0 eV, were observed, corresponding to C═C/C−C in aromatic rings, C−O, C═O, and COOH groups, respectively. After the reduction, the intensities of the oxygen-containing functional groups were greatly weakened. On the basis of the XPS data, the oxygen content decreased from 31% in graphene oxide to 12% in reduced graphene oxide.

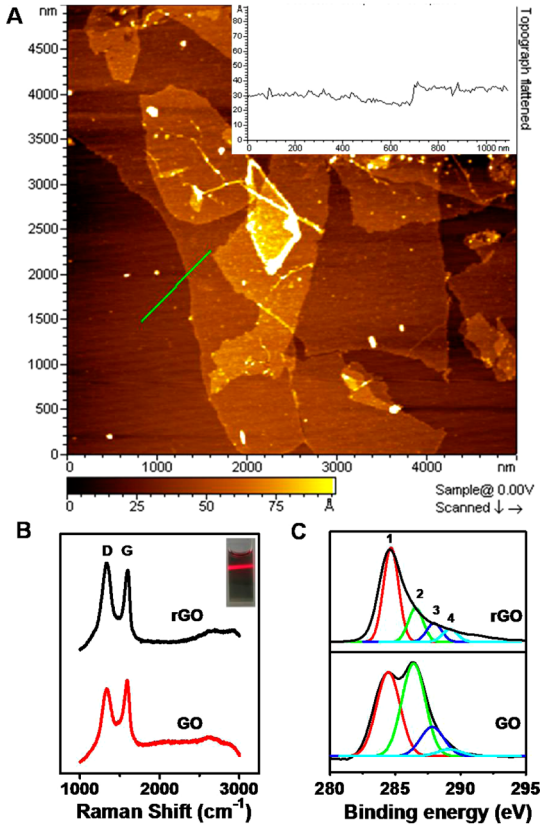

Figure 1. (A) Typical AFM image and height profile of in-house prepared graphene oxide on freshly cleaved mica substrate. (B) Raman spectra and (C) high-resolution C 1s spectra of graphene oxide and reduced graphene oxide. The peaks correspond to (1) C═C/C−C in aromatic rings, (2) C−O, (3) C═O, and (4) COOH groups, respectively. The inset in (B) shows the Tyndall effect of reduced graphene oxide.

Benefiting from the residual oxygen-containing functional groups, the thus-prepared reduced graphene oxide was well-dispersed in aqueous solution, which is similar to graphene dispersions prepared by hydrothermal reduction and hydrazine reduction.[30,32] This can be attributed to the electrostatic repulsion between ionized reduced graphene oxide sheets. The colloidal nature of the resultant reduced graphene oxide can be further confirmed by the observed Tyndall effect (Figure 1B inset). The stable colloidal state makes the reduced graphene oxide useful as a sensing element for developing homogeneous assays.

The working principle of our design is illustrated in Figure 2A. The sensing platform features reduced graphene oxide as a transducing mediator and an ssDNA probe that contains two important sequence domains: a 3′ domain that acts as the primer to initiate RCA (through the binding of a circular DNA template) and a 5′ domain made of an aptamer as the molecular recognition element. Upon mixing, the DNA probe is expected to adsorb onto the reduced graphene oxide surface due to strong DNA−graphene $\pi-\pi$ stacking interactions. The formation of the DNA-reduced graphene oxide conjugate serves to mask the primer domain, making it unavailable for RCA. However, since it is known that graphene-adsorbed aptamers can undergo conformation changes upon target binding,[16−18] it is anticipated that the adsorbed probe will be released from the reduced graphene oxide surface in the presence of the target for the aptamer, liberating the primer domain for RCA. The detection of the target for the aptamer is therefore easily converted to detection of the RCA products.

To validate the above design, we set out to engineer a sensing system for thrombin. Following an optimization experiment to determine a suitable length of the primer domain (to be discussed below), we obtained a functional thrombin probe, named TP1, with the following sequence: 5′-**GGTTG GTGTG GTTGG** AA*CAG TCAGT CAGT*-3′. The probe contains 29 nucleotides, distributed as the antithrombin aptamer (bold letters) at the 5′ end,[33,34] the primer for RCA (italic letters) at

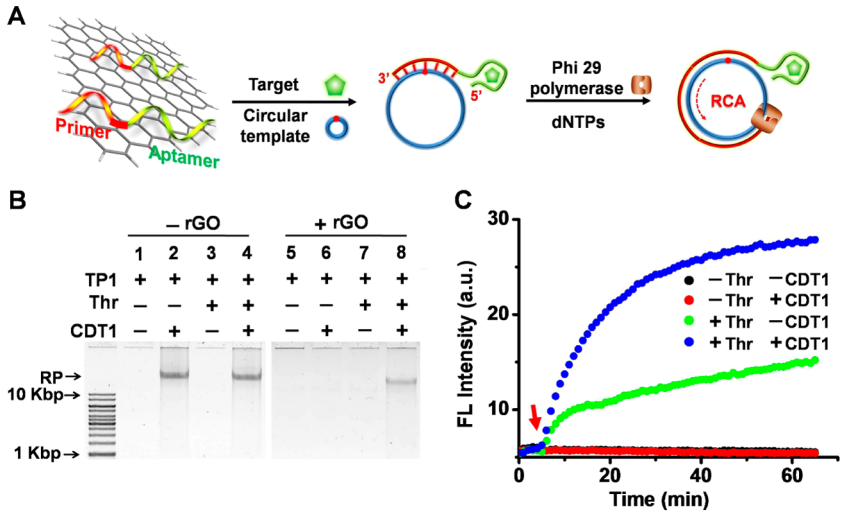

Figure 2. (A) Schematic representation of reduced graphene oxide-aptamer-RCA biosensing platform. (B) Analysis of RCA products (RP) by 0.6% agarose gel electrophoresis. Each reaction was performed for 1 h at 30 °C in 60 μL of target binding buffer (TBB: 20 mM PBS, 150 mM NaCl, 20 mM KCl, 5 mM $MgCl_2$, pH 7.5) containing indicated components of reduced graphene oxide-adsorbed TP1 (250 nM), CDT1 (8 nM), and thrombin (Thr; 200 nM). (C) Time-dependent fluorescence response of reduced graphene oxide-adsorbed FAM-labeled TP1 (250 nM) in the presence of Thr (200 nM), CDT1 (8 nM), or both. $\lambda_{ex}/\lambda_{em}$ = 494/518 nm.

the 3′ end, and a 2-nucleotide spacer in between (underlined letters). Agarose gel analysis indicates that in the absence of reduced graphene oxide, a significant amount of RCA products was produced when TP1 was incubated with CDT1 (the circular template used in this study; its sequence is given in Table S1 in Supporting Information), dNTPs and phi29 DNA polymerase (DNAP) both with (Figure 2B, lane 4) and without thrombin (lane 2). In addition, RCA products were not observed when CDT1 was omitted (lane 1, without thrombin; lane 3, with thrombin). These control experiments showed that the aptamer-tagged primer was still able to initiate the RCA reaction.

TP1 was then allowed to adsorb onto the reduced graphene oxide surface (see Experimental Section for experimental details) and the assembled TP1-reduced graphene oxide hybrid was then used for the RCA reaction in the presence of thrombin only (lane 7), CDT1 only (lane 6) or both (lane 8). RCA products were not produced when only CDT1 or thrombin was supplied. However, RCA products were observed when both CDT1 and thrombin were provided. These results are consistent with the proposed mechanism shown in Figure 2A: (1) the strong DNA-reduced graphene oxide interaction prevents the primer domain of TP1 from hybridizing to CDT1 to initiate RCA; (2) the addition of the target is able to reactivate RCA, presumably through the release of TP1 from the reduced graphene oxide surface.

A kinetic experiment was performed to record the time-dependent fluorescence changes of 5′ FAM-labeled TP1 (F-TP1) after exposure to various amounts of reduced graphene oxide in order to determine the concentration of reduced graphene oxide required to adsorb 250 nM TP1. The maximal fluorescence quenching was observed when reduced graphene oxide reached 8 μg/mL (Figure S1A). It should be noted that we also compared the quenching ability of reduced graphene oxide to that of graphene oxide and the data in Figure S1B shows that reduced graphene oxide exhibited significantly better quenching efficiency than graphene oxide.

We then examined time-dependent fluorescence changes of reduced graphene oxide-adsorbed F-TP1 in the presence of thrombin, CDT1, or both. As shown in Figure 2C, CDT1 was unable to cause the detachment of the adsorbed TP1, reflected by the lack of fluorescence enhancement over time. However, thrombin caused a gradual increase of fluorescence intensity, implying that TP1 was slowly liberated from reduced graphene oxide surface. To our surprise, simultaneous addition of both thrombin and CDT1 resulted in a more dramatic increase of fluorescence. This observation indicates that CDT1 and thrombin have a synergistic effect on the desorption of TP1 from the reduced graphene oxide surface. Also of note, the interaction between the primer and template was sequence-specific. It was observed that CDT1 induced a much higher level fluorescence from the reduced graphene oxide-adsorbed, 5′ FAM-labeled DNA probe with a fully matched sequence than those with 1–4 mismatches (Figure S2). This specificity was similar to that of a graphene-based molecular beacon for DNA detection.[12,36]

The implementation of our strategy relies on the use of two sequence elements in a single DNA probe: a short primer element at the 3′ end (to hybridize to the circular template) and the molecular recognition element at the 5′ end (for target binding). To examine the target-dependent amplification on the degree of

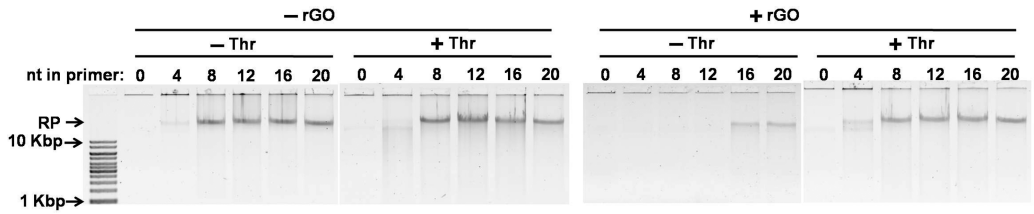

Figure 3. RCA reactions using thrombin probes with a primer domain of 0, 4, 8, 12, 16, and 20 nucleotides (nt). RCA was performed at 30 °C for 1 h in 60 μL of 1× RCA reaction buffer containing 250 nM reduced graphene oxide-adsorbed probe, 8 nM CDT1, 500 nM dNTPs, and 1 U DNAP.

primer-template complementarity, we tested several probes that consisted of the same antithrombin aptamer but a variable primer sequence carrying 0, 4, 8, 12, 16, and 20 nucleotides (their sequences are provided in Table S1). Each probe was first allowed to bind to reduced graphene oxide. The adsorption was completed in 30 min for all the probes independent of their lengths (Figure S3). Once the probe-reduced graphene oxide hybrid was formed, it was then employed in the RCA reaction. As shown in Figure 3, in the absence of reduced graphene oxide, RCA proceeded with and without thrombin for the probes carrying 8, 12, 16, and 20 nucleotides in the primer domain. In the presence of reduced graphene oxide, however, the probes with 8 and 12 nucleotides were able to carry out thrombin-dependent RCA. Further extending the primer length to 16 and 20 nucleotides led to higher background RCA (thrombin-independent RCA), probably as a result of the formation of more stable primer-template duplex that competed well with probe-reduced graphene oxide interactions. This is also consistent with previous findings that the amount of desorption was larger for the longer DNA targets.[35,36]

The effect of the CDT1 concentration on the RCA reaction of TP1 was evaluated next for the consideration that high template concentrations may cause the release of the adsorbed TP1 from the reduced graphene oxide surface and can thus lead to target-independent RCA (background RCA). RCA products were not generated with the increase of CDT1 concentration from 3.2 to 80 nM (Figure S4). However, substantial amounts of RCA products were formed at higher concentrations, implying that high CDT1 concentrations can indeed promote desorption of TP1. The effect of RCA reaction time on the RCA product production was also examined. Increasing the reaction time led to increasing amounts of RCA products (Figure S5). We chose 1 h as the RCA reaction time as it was relatively short and the amount of RCA products was quite substantial.

With the establishment of optimal experimental conditions for target-dependent RCA, we carried out three experiments to examine TP1-reduced graphene oxide binding and the synergistic displacement of TP1 by thrombin and CDT1 in more details using 5′-^{32}P-labeled TP1. The use of radioactive TP1 facilitated the analysis of the distribution of reduced graphene oxide-adsorbed TP1 and unbound TP1 in solution: each sample was simply centrifuged to precipitate reduced graphene oxide, followed by dPAGE analysis to determine the percentage of TP1 in the supernatant (S) and the precipitant (P).

In the first experiment (Figure 4A), 250 nM TP1 was premixed with 4, 8, 12, and 16 μg/mL reduced graphene oxide for 1 h, followed by incubation with 80 nM CDT1 for 2 h. When reduced graphene oxide was used at 4 μg/mL, TP1 was distributed almost equally in P and S fractions (lanes 3 and 4). The TP1-reduced graphene oxide complex appeared to be highly stable and did not undergo detectable exchange with subsequently added CDT1 (100% of CDT1 was found in the supernatant; lanes 5 and 6). When the concentration of reduced graphene oxide was increased to 8, 12, and 16 μg/mL, TP1 was found exclusively in the P fraction (comparing lanes 7 and 8; 11 and 12; 15 and 16) but more and more CDT1 became adsorbed by reduced graphene oxide (comparing lanes 9 and 10; 13 and 14; 17 and 18). At 16 μg/mL reduced graphene oxide, CDT1 were found entirely in the P fraction. Reduced graphene oxide at 8 μg/mL was deemed to be an ideal setting for the RCA reaction because TP1 was completely adsorbed by the nanomaterial while most of the CDT1 molecules were not adsorbed by reduced graphene oxide and available as the circular template for RCA.

The second experiment was conducted to assess the time required to achieve the complete adsorption of 250 nM TP1 by 8 μg/mL reduced graphene oxide. The data presented in Figure 4B show that the adsorption was completed in 1 h.

The release of TP1 from the surface of reduced graphene oxide by thrombin, CDT1 or both was analyzed in the third experiment. Once again, premixing TP1 (250 nM) and reduced graphene oxide (8 μg/mL) led to complete TP1 adsorption (lanes 3 and 4; Figure 4C). The addition of thrombin (600 nM) resulted in 30% release of TP1 into supernatant (comparing lanes 5 and 6) while the addition of CDT1 (80 nM) alone did not cause any detectable amount of TP1 release (lanes 7 and 8). However, simultaneous addition of thrombin and CDT1 resulted in significantly enhanced release of TP1 (comparing lanes 6 and 10; 30% *vs* 55%

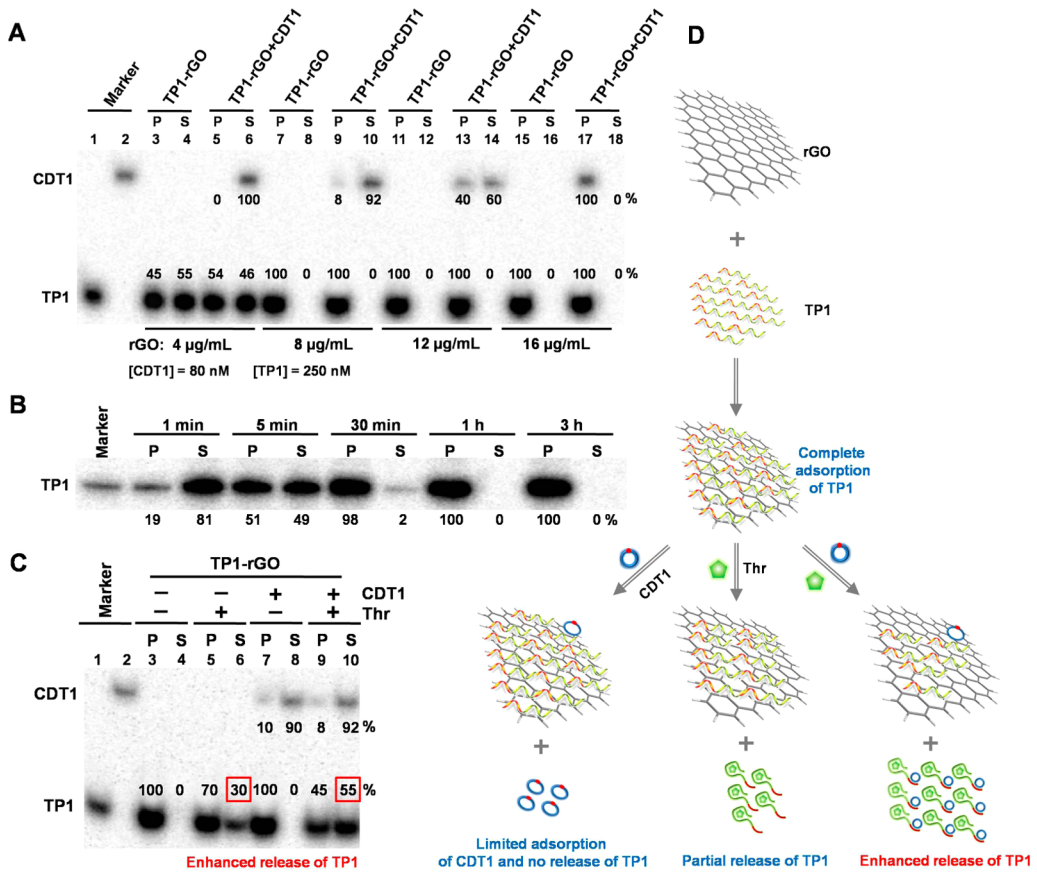

Figure 4. Analysis of DNA-reduced graphene oxide binding and dissociation using radioactive DNA probes. (A) Binding of CDT1 to reduced graphene oxide (rGO) premixed with TP1. Radioactive TP1 (250 nM) was mixed with a specific concentration of reduced graphene oxide (4, 8, 12, or 16 μg/mL) for 1 h, followed by incubation with radioactive CDT1 (80 nM) for 2 h. Reduced graphene oxide was then separated from the solution by centrifugation; TP1 and/or CDT1 in the precipitant (P) and supernatant (S) were analyzed by 10% dPAGE. (B) Kinetic analysis of TP1-reduced graphene oxide binding. Radioactive TP1 (250 nM) and reduced graphene oxide (8 μg/mL) were incubated for 1, 5, 30, 60, and 180 min prior to centrifugation and dPAGE analysis. (C) Release of TP1 from the reduced graphene oxide surface by thrombin, CDT1 or both. Radioactive TP1 (250 nM) and reduced graphene oxide (8 μg/mL) were incubated for 1 h, followed by incubation with thrombin (600 nM), radioactive CDT1 (80 nM), or both for 2 h prior to centrifugation and dPAGE analysis. (D) Schematic illustration of experimental observations shown in the preceding panels.

of TP1 release), confirming the synergistic effect observed earlier with fluorescently labeled TP1.

The results obtained above are summarized in the mechanistic depiction of the adsorption-release processes (Figure 4D) that are based on the following key findings. (1) Premixing 250 nM TP1 with 8 μg/mL reduced graphene oxide leads to complete adsorption of TP1 onto the surface of reduced graphene oxide. (2) Under this condition, some DNA binding sites are still available, which can result in the adsorption of a small amount of 80 nM CDT1. However, the preadsorbed TP1 does not undergo an exchange reaction with CDT1, which is important for low-background RCA-based biosensing assay. (3) Thrombin competes successfully with reduced graphene oxide for TP1 binding, and as a result, it can cause desorption of TP1 from the reduced graphene oxide surface. (4) Although CDT1 alone cannot displace an appreciable level of TP1 release, it can act as a synergistic partner for thrombin to produce a much-enhanced release of TP1 from the reduced graphene oxide surface.

To demonstrate the analytical utility of the proposed approach, we employed a molecular beacon (MB) to enable fluorescent detection of RCA products (Figure 5A).[37] This method takes advantage of the sensitivity of fluorescence detection, along with the unique homogeneous assaying capability offered by MB probes.[38,39] The sequence of the chosen MB, MB1 (Table S1), was embedded into CDT1 and thus, the resultant RCA products contain repeating sequence units that are complementary to MB1. When mixed with RCA products from thrombin-induced RCA reactions, MB1 was able to produce fluorescent signals proportional to the concentration of thrombin (Figure 5A,B). The assay has a limit of detection (LOD, defined as 3σ, σ = standard deviation of the blank samples) of 10 pM and a linear dynamic range of 10−200 pM (Figure 4C). It is worth noting that the LOD is nearly 2 orders of magnitude lower than that of graphene-based aptamer sensors without amplification under similar detection conditions.[21] It is also about 10 times better than previously

reported amplified fluorescent sensors.[40,41] Agarose gel electrophoresis was also carried out to directly monitor RCA products from the RCA reactions in the presence of increasing concentrations of thrombin (Figure 5D). This method was also able to detect thrombin as low as 10 pM, which was consistent with the fluorescent assay based on MB1.

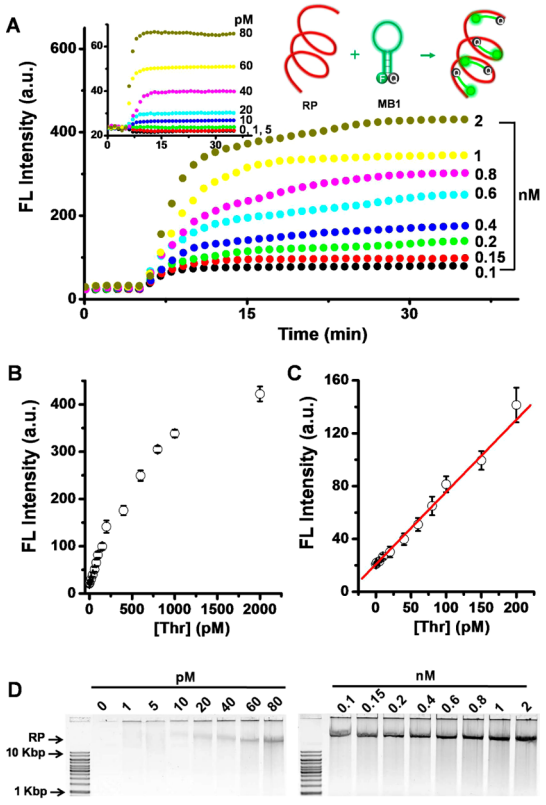

Figure 5. Fluorescence detection of RCA products using the molecular beacon MB1. (A) Time-dependent fluorescence upon incubation of MB1 with RCA products obtained with varying thrombin concentrations. Experiments were carried out at 30 °C in 60 μL of DNA binding buffer (DBB; 20 mM PBS, 150 mM NaCl, 5 mM $MgCl_2$, pH 7.5) containing 1 μM MB1 and 5 μL of the RCA reaction mixture. (B and C) Fluorescence intensity (FL; fluorescence readings at 35 min) as a function of thrombin concentration between 0 and 2000 pM and 0−200 pM, respectively. (D) Analysis of RCA products by agarose gel electrophoresis. The RCA reactions were performed at 30 °C for 1 h in 60 μL of 1× RCA reaction buffer containing 250 nM reduced graphene oxide-adsorbed TP1, 80 nM CDT1, 500 nM dNTPs, 1 U DNAP, and varying concentrations of thrombin indicated in the figure.

To confirm the general applicability of the approach, we designed two additional sensors, one for ATP sensing (Figure 6) and the other for DNA detection (Figure S6). In each case, the original DNA probe TP1 was altered simply through the replacement of the antithrombin aptamer with a new molecular recognition element. The ATP probe, named AP1, contains a well-known anti-ATP aptamer;[42] the DNA probe, DP1, has a specific DNA sequence designed to recognize single-stranded HCV-1 DNA representing a portion of the complementary DNA sequence from the hepatitis C virus genome (the sequences of AP1, DP1 and HCV-1 DNA can be found in Table S1).[31] Once again, the synergistic effect exerted by both the target and the circular DNA template on the release of the probe adsorbed onto the reduced graphene oxide surface was observed (Figure 6A and Figure S6A). Furthermore, the molecular beacon based method was also able to report the target concentration (Figure 6B and Figure S6B). The LOD for the ATP and DNA sensors was found to be 60 nM and 0.8 pM, respectively, comparable or better than previously reported amplified fluorescent sensors for the same target.[20,21,43−48] Taken together, we can conclude that our strategy is generally applicable to many different targets.

Besides the high sensitivity, each sensor also exhibited excellent selectivity for its cognate target (Figure 7). No increase of fluorescence was observed when each system was tested with unintended targets: bovine serum albumin (BSA) for the thrombin sensor (Figure 7A), GTP, CTP and UTP for the ATP sensor (Figure 7B), and HCV-M1 and HCV-M2 for the DNA sensor (Figure 7C).

We next examined the ability of reduced graphene oxide to protect DNA probes from the digestion by

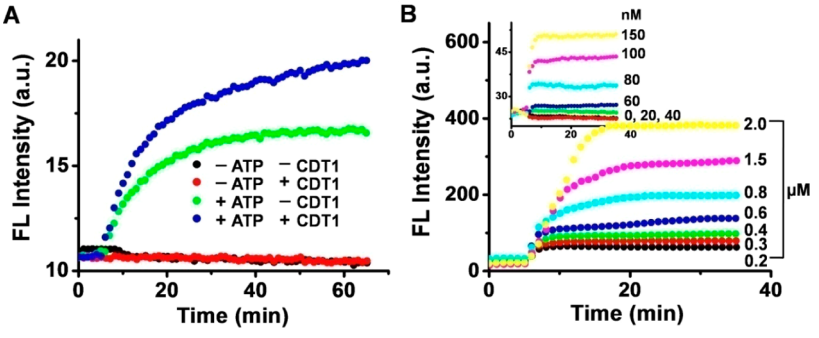

Figure 6. A biosensing system for ATP detection. (A) Time-dependent fluorescence response of reduced graphene oxide-adsorbed FAM-labeled AP1 in the presence of different inputs. Experiments were carried out at 30 °C in 60 μL of TBB containing 200 nM reduced graphene oxide-adsorbed AP1, 8 nM CDT1, 400 μM ATP, or both. (B) Time-dependent fluorescence responses upon incubation of MB1 with RCA products obtained with varying concentrations of ATP. Experiments were carried out under the same conditions as described for Figure 5A.

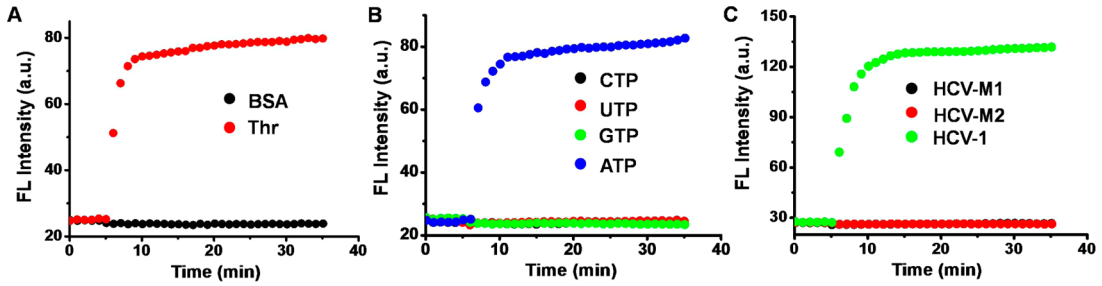

Figure 7. Selectivity of the sensing system for (A) thrombin, (B) ATP, and (C) DNA. RCA was performed at 30 °C for 1 h in 60 μL of 1× RCA reaction buffer containing 250 nM reduced graphene oxide-adsorbed TP1 or DP1, or 200 nM reduced graphene oxide-adsorbed AP1, 80 nM CDT1, 500 nM dNTPs, 1 U DNAP, 0.1 nM thrombin or 10 nM BSA (for panel A), 0.3 μM ATP or 1 μM CTP, UTP, or GTP (for panel B), 8 pM HCV-1 DNA or 0.8 nM HCV-M1 DNA and HCV-M2 DNA (for panel C). Time-dependent fluorescence responses upon mixing MB1 with each RCA reaction mixture were measured under the same conditions as described for Figure 5A.

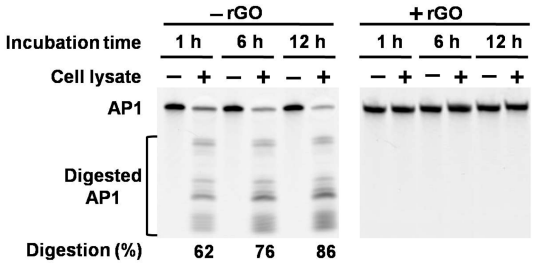

Figure 8. Protection of AP1 by reduced graphene oxide against degradation by nucleases in cell lysates. Radioactive AP1 in the absence and presence of reduced graphene oxide was incubated with cell lysate prepared from MCF-7 for 1, 6, and 12 h prior to dPAGE analysis for the assessment of degradation of AP1 by cellular nucleases.

cellular nucleases. Specifically, AP1 was challenged with cell lysates prepared from MCF-7, a human breast cancer cell line. As shown in Figure 8, increasing amounts of AP1 were digested by cellular nucleases when AP1 was incubated for 1, 6, and 12 h with cell lysate in the absence of reduced graphene oxide, reflected by the reducing band intensity of the original AP and appearance of multiple shortened DNA fragments on the dPAGE gel. As much as 86 ± 7% of free AP1 was digested following 12-h incubation. In stark contrast, reduced graphene oxide was very effective in protecting AP1 from nuclease digestion as no degradation product was observed even after the exposure of AP1-reduced graphene oxide complex to the same cell lysate for 12 h.

With confirmed protection of AP by reduced graphene oxide, we examined the use of AP1-reduced graphene oxide-RCA strategy to detect ATP present in the above cell lysate. As a control, we also carried out ATP detection for the same biological sample set using a commercially available luciferase-based ATP detection kit. The data provided in Table 1 show that both the luciferase assay and our method produced comparable ATP concentrations for cell lysates prepared from three independent MCF-7 cell cultures. This experiment indicates that the use of aptamer-reduced graphene oxide conjugates can achieve detection of target analytes within real biological samples, a task that may not be feasible with unprotected DNA aptamers, which would be digested by cellular nucleases. It is noteworthy that our method consistently produced somewhat higher ATP concentrations than those from the luciferase assay. A likely explanation is that although luciferase is only reactive with ATP, the DNA aptamer also recognizes other adenosine species, such as adenosine, AMP and ADP.[42]

We also challenged the proposed method by analyzing thrombin in a matrix of human serum (Figure 9A). We tested three serum samples with the following dilutions: 1:1, 1:5 and 1:50. At 1:1 dilution, significant background signal was observed, resulted an increased LOD of 200 pM (based on 3σ of the blank). At 5-fold dilution, reduced background signal was observed and the method was able to achieve an LOD of 50 pM. At 50-fold dilution, the background signal dropped to the same level of pure buffer, with an observed LOD of 10 pM. The increased background signal at high concentrations of serum (1:1 and 1:5 dilutions) was most possibly due to nonspecific probe–target interactions. It is noteworthy that 50-fold diluted serum was also used in a previous aptamer sensor study with a reported LOD of 10 pM.[49] These results suggest that the present method could potentially be used for protein detection in biological media, although caution needs to be exercised for background signal.

A notable feature of our DNA detection assay is that it was able to detect HCV-1 DNA in the mixture that also contained HCV-M1 and HCV-M2. A series of DNA samples with varying levels of HCV-1 DNA in the presence of HCV-M1 DNA (1 nM) and HCV-M2 DNA (1 nM) were tested for this experiment (Figure 9B). It was observed that the signal responses were comparable with the samples containing only HCV-1 DNA, and the calculated recovery values ranged from 93% to 115%. These results demonstrated that our approach could potentially be used for the detection of a specific DNA target within a DNA mixture.

TABLE 1. Analysis of ATP in Cell Lysate

biological replicates[a]	bioluminescence assay (μM)[b]	RSD (%)	our assay (μM)	RSD (%)	Extra ATP added (μM)	Bioluminescence assay (μM)[b]	RSD (%)	Our assay (μM)	RSD (%)
1	4.3	9.2	6.2	6.5	5.0	8.7	6.6	12.0	5.3
2	3.6	8.4	5.3	7.8	1.0	3.9	9.8	7.1	7.3
3	2.8	9.6	4.2	8.1	0.5	2.9	8.6	5.2	6.6

[a] Three independent cell lysates were used. [b] The bioluminescence assay involved the use of luciferase and luciferin (Molecular Probes).

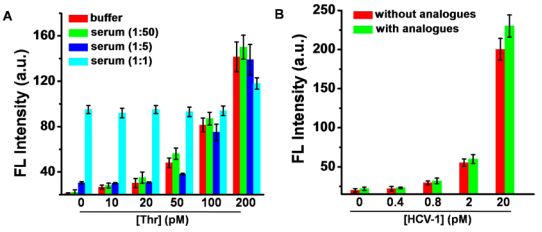

Figure 9. (A) Fluorescence responses upon incubation of MB1 with RCA products obtained with varying thrombin concentrations spiked in 1, 5, 50-fold dilutions of serum samples. (B) Fluorescence responses upon incubation of MB1 with RCA products obtained with varying levels of HCV-1 DNA only (red data series) and HCV-1 DNA in the presence of 1 nM HCV-M1 and 1 nM HCV-M2 (green data series). Experiments were carried out at 30 °C in 60 μL of DBB containing 1 μM MB1 and 5 μL of the RCA reaction mixture.

CONCLUSIONS

In summary, we have developed a versatile biosensing platform that is able to carry out ultrasensitive detection of wide-ranging targets. The system uniquely exploits a nanomaterial (reduced graphene oxide), a biomaterial (DNA aptamers), and an isothermal signal amplification technique (RCA). Reduced graphene oxide is chosen for its ability to adsorb single-stranded DNA molecules nonspecifically. DNA aptamers are selected for their ability to bind reduced graphene oxide but undergo target-induced conformational changes that facilitate their release from the reduced graphene oxide surface. RCA is employed for its ability to amplify a primer-template recognition event into repetitive sequence units that can be easily detected. Tagging a relatively short primer to an aptamer sequence is considered key to the design: the relatively small DNA probe allows for both effective probe adsorption onto the reduced graphene oxide surface to mask the primer domain in the absence of the target as well as efficient probe release in the presence of the target to make the primer available for template binding and RCA. To the best of our knowledge, the described strategy has never been reported before. We also made an observation that the circular template, which on its own does not cause a detectable level of probe release from the reduced graphene oxide surface, augments target-induced probe release. Although the precise reason for the observed synergistic effect has yet to be fully investigated, we speculate that the cooperativity may reflect that the aptamer-target tertiary structure formation may tip the balance from the probe-reduced graphene oxide binding to the probe-template hybridization. We further speculate that the synergy helps promote the release of a small amount of probe from the reduced graphene oxide surface at extremely low concentrations of the target, which is then captured by the circular template for signal amplification. Considering the high detection sensitivity and broad target applicability, we envision that the described biosensing platform will find useful applications in biological, medical, and environmental fields.

EXPERIMENTAL SECTION

Oligonucleotides and Other Materials. All DNA oligonucleotides (Table S1) were obtained from Integrated DNA Technologies (IDT), and purified by standard 10% denaturing (8 M urea) polyacrylamide gel electrophoresis (dPAGE). Adenosine 5′-triphosphate (ATP), T4 DNA ligase, and phi29 DNA polymerase (DNAP) were purchased from MBI Fermentas (Burlington, Canada). γ-[^{32}P]ATP was purchased from PerkinElmer. Human serum (male, type AB) and all other chemicals were purchased from Sigma-Aldrich (Oakville, Canada) and used without further purification. Water was purified with a Milli-Q Synthesis A10 water purification system.

Instruments. Fluorescence measurements were performed with a Cary Eclipse fluorescence spectrophotometer (Varian) with an excitation wavelength (λ_{ex}) of 494 nm and an emission wavelength (λ_{em}) of 518 nm. The bandpasses for excitation and emission were set at 5 and 10 nm, respectively. Photomultiplier tube voltage was set at 600 V. Fluorescence images of dPAGE gels were obtained using a Typhoon 9200 variable mode imager (GE Healthcare). Atomic force microscopy (AFM) measurements were carried out on Agilent PicoPlus II. Raman spectra were recorded on a Renishaw Micro-Raman system 2000 spectrometer with He−Ne laser excitation (623.8 nm). X-ray photoelectron spectroscopy (XPS) was performed with a VG ESCALAB 250 spectrometer using anonmonochromatized Al KR X-ray source (1486.6 eV).

Preparation of Circular DNA Template (CDT1). A total of 600 pmol of phosphorylated linear CDT1 was first mixed with 700 pmol of DP1 (DNA primer for templated DNA ligation) in 45 μL of H_2O, heated to 90 °C for 3 min, and cooled to room temperature for 15 min. To this mixture were added 5 μL of 10× T4 DNA ligase buffer and 10 U (U: unit) T4 DNA ligase, and the resultant mixture was incubated at room temperature for 1 h before heating at 90 °C for 5 min to deactivate the ligase. The ligated circular DNA molecules were concentrated by standard ethanol precipitation and purified by dPAGE.

Target Detection. In a typical thrombin detection experiment, 450 μL of target binding buffer (TBB; 20 mM PBS, 150 mM NaCl, 20 mM KCl, 5 mM $MgCl_2$, pH 7.5), 10 μL of 15 μM TP1, and 40 μL of 100 μg/mL reduced graphene oxide solution were incubated

at 30 °C for 30 min. Then, 50 μL of the above stock solution was transferred into a 1.5 mL microcentrifuge tube. Subsequently, 2 μL of thrombin stock solution (0−300 nM) and 1 μL of CDT1 (4.8 μM) were added. Following 1 h incubation at 30 °C, 6 μL of 10× RCA reaction buffer (330 mM Tris acetate, 100 mM magnesium acetate, 660 mM potassium acetate, 1% (v/v) Tween-20, 10 mM DTT, pH 7.9), 1 U of DNAP, and 1 μL of dNTPs (with a final concentration of 500 μM) were introduced to the above mixture (total volume: 60 μL). The reaction mixture was incubated at 30 °C for 1 h before heating at 65 °C for 15 min. Finally, 5 μL of RCA products from the above reaction mixture was added into 55 μL of DNA binding buffer (DBB; 20 mM PBS, 150 mM NaCl, 5 mM $MgCl_2$, pH 7.5) containing 1 μM molecular beacon MB1 in a cuvette with a constant temperature at 30 °C. Time-dependent fluorescence at $\lambda_{ex}/\lambda_{em}$ = 494/518 nm was recorded.

The procedure for ATP detection was similar to that for the thrombin detection except that the reagents were used as follows: 10 μL of 12 μM AP1 stock solution, 1 μL of CDT1 (0.96 μM), and 2 μL of ATP stock solution (0−200 μM).

The procedure for the HCV DNA detection was similar to that for the thrombin detection except that the reagents were used as follows: 450 μL of DBB, 10 μL of 15 μM DP1 stock solution, and 2 μL of single-stranded HCV-1 DNA stock solution (0−10 nM).

Release of Radioactive TP1 from the Reduced Graphene Oxide Surface by Thrombin and Radioactive CDT1. TP1 and CDT1 were first labeled with γ-[^{32}P]ATP at the 5′ end using T4 polynucleotide kinase according to the manufacturer's protocol, and purified by 10% dPAGE. For the reaction in Figure 4A, 250 nM of TP1 was incubated with 4, 8, 12, and 16 μg/mL reduced graphene oxide in 1× TBB at 30 °C for 1 h, followed by addition of CDT1 to 80 nM and further incubation at 30 °C for 2 h. Each mixture was then centrifuged at 15 000*g* for 20 min at 4 °C. The resultant precipitate and supernatant were analyzed by 10% dPAGE. For the reactions in Figure 4B, 250 nM TP1 was incubated with 8 μg/mL reduced graphene oxide in 1× TBB at 30 °C for 1, 5, 30, 60, and 180 min prior to centrifugation and dPAGE analysis. Experiments in Figure 4C were carried out similarly to Figure 4A except that (1) reduced graphene oxide was used at 8 μg/mL and (2) 600 nM thrombin was used for the release reaction.

Cell Culture and Cell Lysate Preparation. The adherent breast cancer cell line MCF-7 was cultured in α-MEM media (GIBCO) supplemented with 10% fetal bovine serum (Invitrogen). Cell cultures were incubated at 37 °C in a humidified incubator maintained at 5% CO_2. Cell lysates were prepared by the following method. Cells were grown to approximately 80% confluence before harvesting, media was removed, and cells were washed with PBS. Cells were coated with 1 mL of a 0.05% trypsin−EDTA solution (Invitrogen) and the excess was removed. Cells were incubated at 37 °C for 5 min to dissociate cells. Dissociated cells were suspended in 1 mL of PBS and pelleted by centrifugation at 3000*g* for 5 min. Supernatant was removed, and cells were resuspended in another 1 mL of PBS and pelleted a second time. After removing the supernatant, the cell pellet was resuspended in 1 mL of 20 mM Tris buffer (pH 7.0) and a fraction was taken for cell counting. Proteoblock protease inhibitor cocktail (Thermo Scientific) was added to the cell suspension at 1× final concentration. The cells were lysed by passage through a 25-gauge needle 10 times. A fraction of the cell lysate was taken for cell counting to ensure complete lysis.

Stability of Reduced Graphene Oxide-Adsorbed AP1 in Cell Lysate. A total of 200 nM FAM-labeled AP1 probe was first mixed with 8 μg/mL reduced graphene oxide in 25 μL of 1× TBB at 30 °C for 1 h. Then, 15 μL of freshly prepared cell lysate was added and incubated at 30 °C for 1, 6, and 12 h. Afterward, the mixtures were heated to 90 °C for 10 min and analyzed by dPAGE. For the control samples, no reduced graphene oxide was added.

ATP Assay in Cell Lysate. Three freshly prepared cell lysate replicates were taken and individually filtered through 0.45 μm membrane (NANOSEP OMEGA, Pall Incorporation). The filtrates were analyzed for ATP concentrations using the AP1/reduced graphene oxide/RCA assay described above. For comparison, ATP levels were also measured with the commercially available ATP Determination Kit (A22066; Molecular Probes), according to the manufacturer's protocol.

Conflict of Interest: The authors declare no competing financial interest.

Acknowledgment. Funding for this work was provided by a Natural Sciences and Engineering Council of Canada Discovery Grant (Y.L.) and the Canada Foundation for Innovation. Part of the work was conducted at the McMaster Biointerfaces Institute.

Supporting Information Available: Preparation of graphene oxide and reduced graphene oxide, oligonucleotide sequences, reduced graphene oxide amount optimization, RCA reaction optimization, agarose gel electrophoresis of RCA products, ssDNA detection and sensing selectivity. This material is available free of charge *via* the Internet at http://pubs.acs.org.

REFERENCES AND NOTES

1. Rosi, N. L.; Mirkin, C. A. Nanostructures in Biodiagnostics. *Chem. Rev.* **2005**, *105*, 1547–1562.
2. Saha, K.; Agasti, S. S.; Kim, C.; Li, X.; Rotello, V. M. Gold Nanoparticles in Chemical and Biological Sensing. *Chem. Rev.* **2012**, *112*, 2739–2779.
3. Wang, H.; Yang, R.; Yang, L.; Tan, W. Nucleic Acid Conjugated Nanomaterials for Enhanced Molecular Recognition. *ACS Nano* **2009**, *3*, 2451–2460.
4. Chen, D.; Feng, H.; Li, J. H. Graphene Oxide: Preparation, Functionalization, and Electrochemical Applications. *Chem. Rev.* **2012**, *112*, 6027–6053.
5. Feng, L. Y.; Wu, L.; Qu, X. G. New Horizons for Diagnostics and Therapeutic Applications of Graphene and Graphene Oxide. *Adv. Mater.* **2013**, *25*, 168–186.
6. Chung, C.; Kim, Y. K.; Shin, D.; Ryoo, S. R.; Hong, B. H.; Min, D. H. Biomedical Applications of Graphene and Graphene Oxide. *Acc. Chem. Res.* **2013**, *46*, 2211–2224.
7. Morales-Narváez, E.; Merkoçi, A. Graphene Oxide as an Optical Biosensing Platform. *Adv. Mater.* **2012**, *24*, 3298–3308.
8. Loh, K. P.; Bao, Q.; Eda, G.; Chhowalla, M. Graphene Oxide as a Chemically Tunable Platform for Optical Applications. *Nat. Chem.* **2010**, *2*, 1015–1024.
9. Wang, Y.; Li, Z.; Wang, J.; Li, J.; Lin, Y. Graphene and Graphene Oxide: Biofunctionalization and Applications in Biotechnology. *Trends Biotechnol.* **2011**, *29*, 205–212.
10. Varghese, N.; Mogera, U.; Govindaraj, A.; Das, A.; Maiti, P. K.; Sood, A. K.; Rao, C. N. R. Binding of DNA Nucleobases and Nucleosides with Graphene. *ChemPhysChem* **2009**, *10*, 206–210.
11. Lu, C. H.; Yang, H. H.; Zhu, C. L.; Chen, X.; Chen, G. N. A Graphene Platform for Sensing Biomolecules. *Angew. Chem., Int. Ed.* **2009**, *48*, 4785–4787.
12. He, S.; Song, B.; Li, D.; Zhu, C.; Qi, W.; Wen, Y.; Wang, L.; Song, S.; Fang, H.; Fan, C. A Graphene Nanoprobe for Rapid, Sensitive, and Multicolor Fluorescent DNA Analysis. *Adv. Funct. Mater.* **2010**, *20*, 453–459.
13. Tang, Z.; Wu, H.; Cort, J.; Buchko, G.; Zhang, Y.; Shao, Y.; Aksay, I.; Liu, J.; Lin, Y. Constraint of DNA on Functionalized Graphene Improves its Biostability and Specificity. *Small* **2010**, *6*, 1205–1209.
14. Dong, H. F.; Ding, L.; Yan, F.; Ji, H. X.; Ju, H. X. The Use of Polyethylenimine-Grafted Graphene Nanoribbon for Cellular Delivery of Locked Nucleic Acid Modified Molecular Beacon for Recognition of MicroRNA. *Biomaterials* **2011**, *32*, 3875–3882.
15. Zhao, X. H.; Kong, R. M.; Zhang, X. B.; Meng, H. M.; Liu, W. N.; Tan, W. H.; Shen, G. L.; Yu, R. Q. Graphene DNAzyme Based Biosensor for Amplified Fluorescence "Turn-On" Detection of Pb^{2+} with a High Selectivity. *Anal. Chem.* **2011**, *83*, 5062–5066.
16. Wang, Y.; Li, Z. H.; Hu, D. H.; Lin, C. T.; Li, J. H.; Lin, Y. H. Aptamer/Graphene Oxide Nanocomplex for *In Situ* Molecular Probing in Living Cells. *J. Am. Chem. Soc.* **2010**, *132*, 9274–9276.
17. Wang, L.; Zhu, J.; Han, L.; Jin, L.; Zhu, C.; Wang, E.; Dong, S. Graphene-Based Aptamer Logic Gates and Their Application to Multiplex Detection. *ACS Nano* **2012**, *6*, 6659–6666.

18. Chang, H.; Tang, L.; Wang, Y.; Jiang, J.; Li, J. Graphene Fluorescence Resonance Energy Transfer Aptasensor for the Thrombin Detection. *Anal. Chem.* **2010**, *82*, 2341–2346.
19. Jang, H. J.; Kim, Y. K.; Kwon, H. M.; Yeo, W. S.; Kim, D. E.; Min, D. H. A Graphene-Based Platform for the Assay of Duplex-DNA Unwinding by Helicase. *Angew. Chem., Int. Ed.* **2010**, *49*, 5703–5707.
20. Lu, C. H.; Li, J.; Lin, M. H.; Wang, Y. W.; Yang, H. H.; Chen, X.; Chen, G. N. Amplified Aptamer-Based Assay through Catalytic Recycling of the Analyte. *Angew. Chem., Int. Ed.* **2010**, *49*, 8454–8457.
21. Liu, X.; Aizen, R.; Freeman, R.; Yehezkeli, O.; Willner, I. Multiplexed Aptasensors and Amplified DNA Sensors Using Functionalized Graphene Oxide: Application for Logic Gate Operations. *ACS Nano* **2012**, *6*, 3553–3563.
22. Cui, L.; Chen, Z.; Zhu, Z.; Lin, X.; Chen, X.; Yang, C. J. Stabilization of ssRNA on Graphene Oxide Surface: An Effective Way to Design Highly Robust RNA Probes. *Anal. Chem.* **2013**, *85*, 2269–2275.
23. Cui, L.; Song, Y.; Ke, G.; Guan, Z.; Zhang, H.; Lin, Y.; Huang, Y.; Zhu, Z.; Yang, C. J. Graphene Oxide Protected Nucleic Acid Probes for Bioanalysis and Biomedicine. *Chem.—Eur. J.* **2013**, *19*, 10442–10451.
24. Connaghan-Jones, K. D.; Moody, A. D.; Bain, D. L. Quantitative DNase Footprint Titration: a Tool for Analyzing the Energetics of Protein-DNA Interactions. *Nat. Protoc.* **2008**, *3*, 900–914.
25. Fire, A.; Xu, S. Rolling Replication of Short DNA Circles. *Proc. Natl. Acad. Sci. U.S.A.* **1995**, *92*, 4641–4645.
26. Zhao, W.; Ali, M. M.; Brook, M. A.; Li, Y. Rolling Circle Amplification: Applications in Nanotechnology and Biodetection with Functional Nucleic Acids. *Angew. Chem., Int. Ed.* **2008**, *47*, 6330–6337.
27. Ali, M. M.; Li, Y. Colorimetric Sensing by Using Allosteric-DNAzyme-Coupled Rolling Circle Amplification and a Peptide Nucleic Acid-Organic Dye Probe. *Angew. Chem., Int. Ed.* **2009**, *48*, 3512–3515.
28. McManus, S. A.; Li, Y. Turning a Kinase Deoxyribozyme into a Sensor. *J. Am. Chem. Soc.* **2013**, *135*, 7181–7186.
29. Tang, L. H.; Liu, Y.; Ali, M. M.; Kang, D. K.; Zhao, W.; Li, J. H. Colorimetric and Ultrasensitive Bioassay Based on a Dual-Amplification System Using Aptamer and DNAzyme. *Anal. Chem.* **2012**, *84*, 4711–4717.
30. Liu, M.; Zhao, H. M.; Chen, S.; Yu, H. T.; Quan, X. Colloidal Graphene as a Transducer in Homogeneous Fluorescence-Based Immunosensor for Rapid and Sensitive Analysis of Microcystin-LR. *Environ. Sci. Technol.* **2012**, *46*, 12567–12574.
31. Liu, M.; Zhao, H. M.; Chen, S.; Yu, H. T.; Quan, X. Interface Engineering Catalytic Graphene for Smart Colorimetric Biosensing. *ACS Nano* **2012**, *6*, 3142–3151.
32. Li, D.; Müller, M. B.; Gilje, S.; Kaner, R. B.; Wallace, G. G. Processable Aqueous Dispersions of Graphene Nanosheets. *Nat. Nanotechnol.* **2008**, *3*, 101–105.
33. Bock, L. C.; Griffin, L. C.; Latham, J. A.; Vermaas, E. H.; Toole, J. J. Selection of Single-Stranded DNA Molecules that Bind and Inhibit Human Thrombin. *Nature* **1992**, *355*, 564–566.
34. Nutiu, R.; Li, Y. Structure-Switching Signaling Aptamers. *J. Am. Chem. Soc.* **2003**, *125*, 4771–4778.
35. Wu, M.; Kempaiah, R.; Huang, P. J. J.; Maheshwari, V.; Liu, J. Adsorption and Desorption of DNA on Graphene Oxide Studied by Fluorescently Labeled Oligonucleotides. *Langmuir* **2011**, *27*, 2731–2738.
36. Huang, P. J. J.; Liu, J. Molecular Beacon Lighting up on Graphene Oxide. *Anal. Chem.* **2012**, *84*, 4192–4198.
37. Nilsson, M.; Gullberg, M.; Dahl, F.; Szuhai, K.; Raap, A. K. Real-time Monitoring of Rolling-Circle-Amplification Using a Modified Molecular Beacon Design. *Nucleic Acids Res.* **2002**, *30*, e66.
38. Tyagi, S.; Kramer, F. R. Molecular Beacons: Probes that Fluoresce upon Hybridization. *Nat. Biotechnol.* **1996**, *14*, 303–308.
39. Wang, K.; Tang, Z.; Yang, C. J.; Kim, Y.; Fang, X.; Li, W.; Wu, Y.; Medley, C. D.; Cao, Z.; Li, J.; *et al.* Molecular Engineering of DNA: Molecular Beacons. *Angew. Chem., Int. Ed.* **2009**, *48*, 856–870.
40. Di Giusto, D. A.; Wlassoff, W. A.; Gooding, J. J.; Messerle, B. A.; King, G. C. Proximity Extension of Circular DNA Aptamers with Real-Time Protein Detection. *Nucleic Acids Res.* **2005**, *33*, e64.
41. Xue, L. Y.; Zhou, X. M.; Xing, D. Sensitive and Homogeneous Protein Detection Based on Target-Triggered Aptamer Hairpin Switch and Nicking Enzyme Assisted Fluorescence Signal Amplification. *Anal. Chem.* **2012**, *84*, 3507–3513.
42. Huizenga, D. E.; Szostak, J. W. A DNA Aptamer That Binds Adenosine and ATP. *Biochemistry* **1995**, *34*, 656–665.
43. Cho, E. J.; Yang, L.; Levy, M.; Ellington, A. D. Using a Deoxyribozyme Ligase and Rolling Circle Amplification To Detect a Non-nucleic Acid Analyte, ATP. *J. Am. Chem. Soc.* **2005**, *127*, 2022–2023.
44. Liu, X.; Freeman, R.; Willner, I. Amplified Fluorescence Aptamer-Based Sensors Using Exonuclease III for the Regeneration of the Analyte. *Chem.—Eur. J.* **2012**, *18*, 2207–2211.
45. Zhang, Z.; Sharon, E.; Freeman, R.; Liu, X.; Willner, I. Fluorescence Detection of DNA, Adenosine-5′-Triphosphate (ATP), and Telomerase Activity by Zinc(II)-Protoporphyrin IX/G-Quadruplex Labels. *Anal. Chem.* **2012**, *84*, 4789–4797.
46. Freeman, R.; Liu, X.; Willner, I. Amplified Multiplexed Analysis of DNA by the Exonuclease III-Catalyzed Regeneration of the Target DNA in the Presence of Functionalized Semiconductor Quantum Dots. *Nano Lett.* **2011**, *11*, 4456–4461.
47. Li, J. W. J.; Chu, Y. Z.; Lee, B. Y. H.; Xie, X. L. S. Enzymatic Signal Amplification of Molecular Beacons for Sensitive DNA Detection. *Nucleic Acids Res.* **2008**, *36*, e36.
48. Wang, F.; Elbaz, J.; Teller, C.; Willner, I. Amplified Detection of DNA through an Autocatalytic and Catabolic DNAzyme-Mediated Process. *Angew. Chem., Int. Ed.* **2011**, *50*, 295–299.
49. Huang, Y.; Chen, J.; Zhao, S.; Shi, M.; Chen, Z.; Liang, H. Label-Free Colorimetric Aptasensor Based on Nicking Enzyme Assisted Signal Amplification and DNAzyme Amplification for Highly Sensitive Detection of Protein. *Anal. Chem.* **2013**, *85*, 4423–4430.